Boson Peak in Deeply Cooled Confined Water: A Possible Way to Explore the Existence of the Liquid-to-Liquid Transition in Water

Zhe Wang,[1] Kao-Hsiang Liu,[1,2] Peisi Le,[1] Mingda Li,[1] Wei-Shan Chiang,[1] Juscelino B. Leão,[3] John R. D. Copley,[3] Madhusudan Tyagi,[3,4] Andrey Podlesnyak,[5] Alexander I. Kolesnikov,[5] Chung-Yuan Mou,[6] and Sow-Hsin Chen[1,*]

[1]*Department of Nuclear Science and Engineering, Massachusetts Institute of Technology, Cambridge, Massachusetts 02139, USA*
[2]*Institute of Atomic and Molecular Sciences, Academia Sinica, Taipei 10617, Taiwan, Republic of China*
[3]*NIST Center for Neutron Research, National Institute of Standards and Technology, Gaithersburg, Maryland 20899, USA*
[4]*Department of Materials Science and Engineering, University of Maryland, College Park, Maryland 20742, USA*
[5]*Spallation Neutron Source, Oak Ridge National Laboratory, Oak Ridge, Tennessee 37831, USA*
[6]*Department of Chemistry, National Taiwan University, Taipei 106, Taiwan, Republic of China*

(Received 24 December 2013; published 12 June 2014)

The boson peak in deeply cooled water confined in nanopores is studied with inelastic neutron scattering. We show that in the (P, T) plane, the locus of the emergence of the boson peak is nearly parallel to the Widom line below ~1600 bar. Above 1600 bar, the situation is different and from this difference the end pressure of the Widom line is estimated. The frequency and width of the boson peak correlate with the density of water, which suggests a method to distinguish the hypothetical "low-density liquid" and "high-density liquid" phases in deeply cooled water.

DOI: 10.1103/PhysRevLett.112.237802 PACS numbers: 61.20.Lc, 63.50.−x

The boson peak is a broad peak observed at low frequencies (~2–10 meV) in the inelastic neutron, x-ray, and Raman scattering spectra of many amorphous materials and supercooled liquids [1–3]. Preliminary measurements on the boson peak in deeply cooled water confined in nanopores [4] and protein surfaces [5] under ambient pressure have been reported. The measured spectra include a boson peak at about 6 meV, which only emerges below ~230 K. A similar result was also observed in a computer simulation study [6]. Since this temperature is close to the ambient-pressure Widom line temperature T_W ~224 K (the Widom line is the locus of specific heat maxima [7]), the authors tentatively explained this phenomenon as due to transformation of the local structure of water from a predominantly high-density liquid (HDL) to a predominantly low-density liquid (LDL) form as T_W is crossed from above. However, this experimental result is insufficient. First, it is clear that this emergence of the boson peak in the raw spectra depends on the energy resolution of the experimental facility. Second, and more importantly, the situation at high pressures has, heretofore, remained unknown. Therefore, without quantitative analysis of the entire spectra, including quasielastic and inelastic components at high pressure, definite conclusions cannot be drawn.

In this Letter, we have measured the boson peak in deeply cooled water with a series of inelastic neutron scattering (INS) experiments in the temperature (T) range from 120 to 230 K and the pressure (P) range from 400 to 2400 bar employing the Disk Chopper Spectrometer (DCS) [8] at the National Institute of Standards and Technology (NIST) Center for Neutron Research and the Cold Neutron Chopper Spectrometer (CNCS) [9] at the Spallation Neutron Source of the Oak Ridge National Laboratory (ORNL). The DAVE software was used for the data reduction [10]. We find that below ~1600 bar, the emergence of the boson peak is correlated (but does not overlap) with the Widom line and with the fragile-to-strong crossover (FSC) in deeply cooled water [11]. Above ~1600 bar, the locus of the emergence of the boson peak in the (P, T) plane has a different slope as compared with its behavior below ~1600 bar, and the end pressure of the Widom line is estimated by determining where the slope begins to change. Moreover, the (P, T) dependences of the shape of the boson peak are found to be related to the density minimum of water [12–14], and a possible way to distinguish the hypothetical LDL phase and HDL phase [15] in deeply cooled water is discussed.

In order to enter the deeply supercooled region of water, we used a nanoporous silica matrix, MCM-41-S, with 15-Å pore diameter to confine the water. When confined, water can remain in the liquid state without crystallization at temperatures much lower than the homogeneous nucleation temperature (~235 K under $P = 1$ bar) [14,16].

The measured energy (E) spectrum at a fixed value of Q (the magnitude of the momentum transfer of the incident neutron) $S_m(Q, E)$ was analyzed using the following equation:

$$S_m(Q,E) = I_{bg}(Q,E) + I_E(Q)R(Q,E) + R(Q,E) \otimes [(I_Q(Q)S_Q(Q,E) + I_I(Q,E)S_I(Q,E))D(E)], \quad (1)$$

where $I_{bg}(Q,E)$ is the background signal from the MCM-41-S matrix, $R(Q,E)$ is the energy resolution function, $I_E(Q)R(Q,E)$ represents the elastic scattering component, $S_Q(Q,E)$ is the quasielastic incoherent dynamic structure factor, $S_I(Q,E)$ is the inelastic incoherent dynamic structure factor, and $D(E)$ is the detailed balance factor [17]. I_Q and I_I are the intensities of the quasielastic and inelastic components, respectively. $S_Q(Q,E)$ represents the diffusive, nonvibrational motions of water molecules and can be modeled using the relaxing cage model (RCM) [18]. In this Letter, the parameters of the RCM are known from previous quasielastic neutron scattering measurements [11,19]. $S_I(Q,E)$ describes the vibrational behavior of water, i.e., the boson peak. Here we use the damped harmonic oscillator (DHO) [20] model to represent $S_I(Q,E)$. The DHO has been used to model various kinds of vibrations, from the self-motion of a single classical damped oscillator to collective excitations in different amorphous materials [20–22]. Using the DHO model, both the frequency and the width of the boson peak can be extracted. Detailed descriptions of the sample, instrument, models, and data analysis can be found in the Supplemental Material [23]. In the following paragraphs, we will present our results and their implications.

The left set of panels in Fig. 1 shows INS spectra $S_m(Q,E)$ measured with the DCS at $Q = 2$ Å^{-1} and corresponding fitted curves under different temperatures and pressures. The right set of panels shows the theoretical incoherent dynamic structure factors extracted from the fit: $S_{th}(Q,E) = n_Q S_Q(Q,E) + n_I S_I(Q,E)$ (n_Q and $n_I = 1\text{-}n_Q$ are the fractional quasielastic and inelastic contributions, respectively). In order to study the relation between the emergence of the boson peak and Widom line crossing in deeply cooled confined water, we first define the emergence of the boson peak as follows: if there is a maximum in the $S_{th}(Q,E)$ curve between ~2 and 10 meV, we state that the boson peak is visible or that the boson peak emerges [e.g., the 200 K case in Fig. 1(b2)]; on the other hand, if the $S_{th}(Q,E)$ curve does not have a maximum, decreasing monotonically in this E range, we state that the boson peak is not visible [e.g., the 225 K case in Fig. 1(b2)]. This definition can be illustrated better if one considers the derivative of $S_{th}(Q,E)$ with respect to E, $\partial_E S_{th}(Q,E)$. A boson peak is observed if $\partial_E S_{th}(Q,E)$ has two roots with $E > 0$ [e.g., the 200 K case in Fig. 2(a1)]; similarly, no peak is observed if $\partial_E S_{th}(Q,E)$ has no roots at $E > 0$ [e.g., the 225 K case in Fig. 2(a1)]. The intermediate condition that $\partial_E S_{th}(Q,E)$ has just one root with $E > 0$, or equivalently, that the maximum value of $\partial_E S_{th}(Q,E)$ [$\max[\partial_E S_{th}(Q,E)]$] just equals 0, corresponds to the critical case that the boson peak just emerges. From the above discussions, it can be found that the emergence or disappearance of the boson peak in the full spectrum is due to the (P, T) dependences of the dynamics of the confined water system, including the slow dynamics [$S_Q(Q,E)$] and the subpicosecond dynamics [$S_I(Q,E)$]. We denote the temperature at which the boson peak just emerges as T_B. In the right column of Fig. 1, we mark the $S_{th}(Q,E)$ curve whose temperature is closest to T_B for each pressure. One

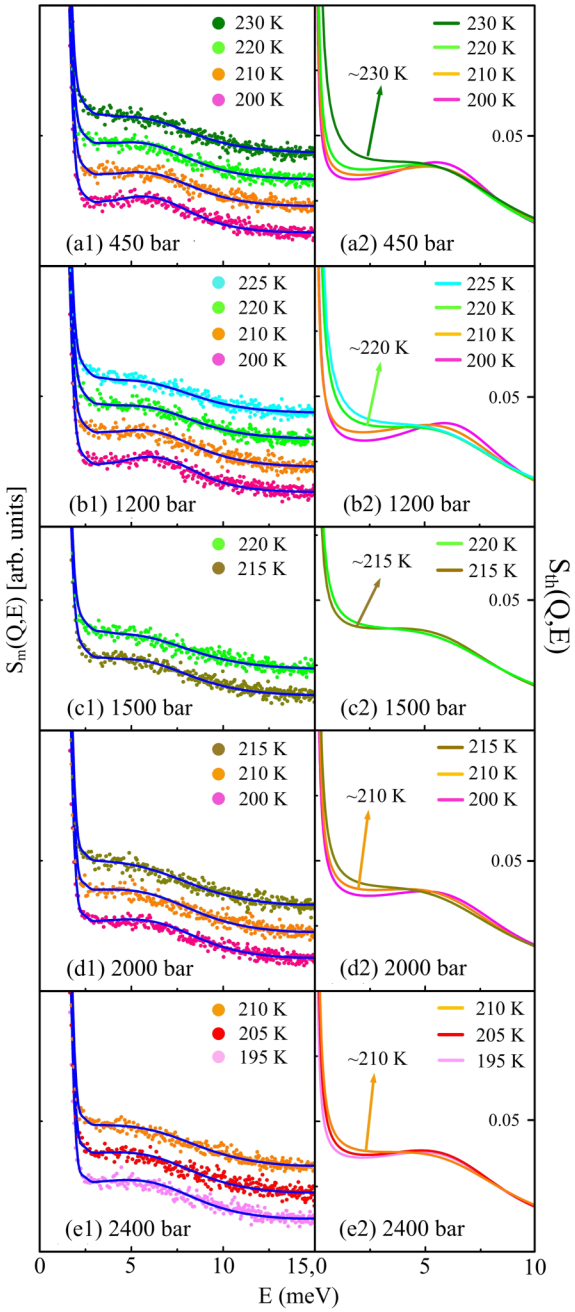

FIG. 1 (color online). INS spectra of the confined water system at $Q = 2$ Å^{-1} at different T and P. For each row, the left panel shows the measured spectrum $S_m(Q,E)$ and corresponding fitted curves under a specific pressure; for clarity, the data have been shifted vertically by a fixed interval between adjacent temperatures. The right panel shows the corresponding theoretical curves $S_{th}(Q,E)$ extracted from the fit. The curve whose temperature is closest to T_B is indicated for each pressure in the right set of panels. (Measured at DCS.)

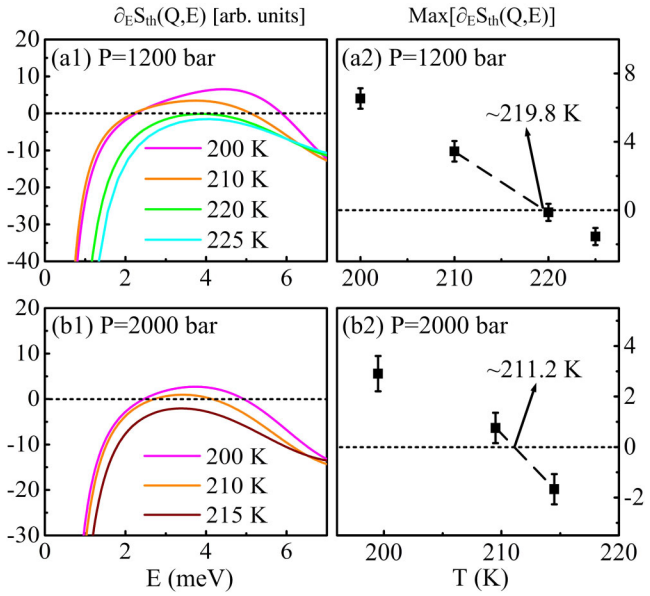

FIG. 2 (color online). An illustration of the definition of T_B. For each row, the left panel shows the derivatives of $S_{th}(Q,E)$ with respect to E, $\partial_E S_{th}(Q,E)$ under a specific pressure. Corresponding maxima of $\partial_E S_{th}(Q,E)$ at different temperatures under this pressure are denoted by squares in the right panel. The linear interpolation method for estimating T_B is illustrated in the right panel.

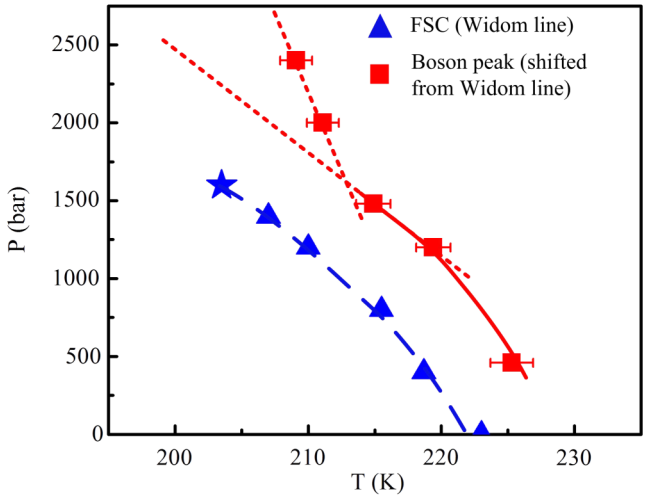

FIG. 3 (color online). $T_B(P)$ in the (P, T) plane. The squares represent interpolated estimates of $T_B(P)$. The triangles demarcate the FSC transition. The star denotes the estimated location of the LLCP obtained from the FSC measurements [11,19]. The two dotted lines denote the extrapolations of the two points at $P = 2000$ and 2400 bar and of the two points at $P = 1200$ and 1500 bar.

may estimate the value of T_B better with a linear interpolation method. Take the 1200 bar case, for example; from Fig. 2(a2), it is found that the value of $\max[\partial_E S_{th}(Q,E)]$ changes smoothly and monotonically as T changes; therefore, one can perform a linear interpolation with respect to $\max[\partial_E S_{th}(Q,E)]$ and T to find out the approximate value of T_B at which $\max[\partial_E S_{th}(Q,E)]$ vanishes. With this method, we obtain $T_B = 219.8 \pm 1.3$ K under 1200 bar, as shown in Fig. 2(a2). Another example is provided by Fig. 2(b2) where T_B is estimated to be 211.2 ± 1.2 K under 2000 bar.

The values of T_B obtained using the method just described are denoted by squares in Fig. 3. The FSC temperatures T_X at different pressures are also shown (as triangles) [11,19]. One can find that below ~1600 bar, the solid curve, which represents the behavior of $T_B(P)$, is nearly parallel to the blue dashed curve that represents the profile of $T_X(P)$. Computer simulation studies suggest that for water models displaying a liquid-liquid critical point (LLCP [15]), the FSC coincides with the Widom line [7]. Thus, we conclude that below ~1600 bar, the emergence of the boson peak has similar P dependence as the Widom line in the sense of the LLCP hypothesis, even though they do not overlap.

Figure 4 shows the extracted frequency (Ω) and full width at half maximum height (Γ) of $S_I(Q,E)$, i.e., the boson peak, as a function of T and P at $Q = 2$ Å^{-1}. Below ~1600 bar, crossing the Widom line, both Ω and Γ change slightly and smoothly. The inset shows that such smooth changes make the boson peak less sharp as T increases. In addition, the quasielastic peak broadens, and its wing is strengthened with increasing T due to a decrease in the translational relaxation time of water molecules $\langle \tau_T \rangle$. Both of these phenomena contribute to the invisibility of the boson peak in the entire spectrum as T increases. Notice that, when crossing the Widom line temperature T_W from

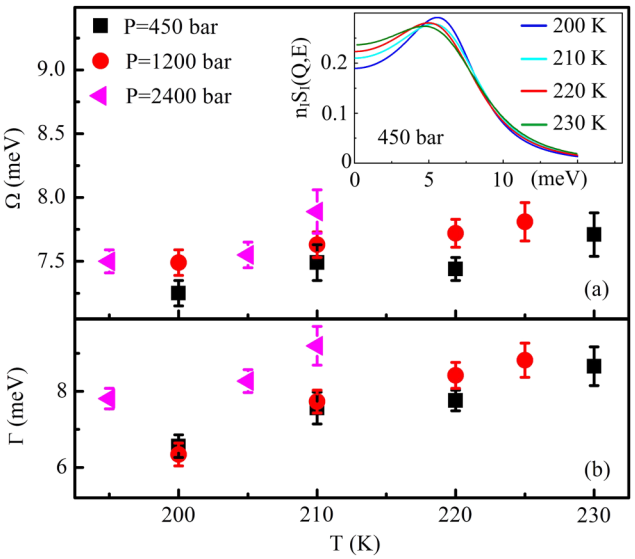

FIG. 4 (color online). (a) Frequency Ω and (b) width Γ of the boson peak at $Q = 2$ Å^{-1} under 450, 1200, and 2400 bar. The temperature range is from 195 to 230 K. The inelastic scattering component $n_I S_I(Q,E)$, which represents the boson peak at $Q = 2$ Å^{-1} under 450 bar, is shown in the inset [24].

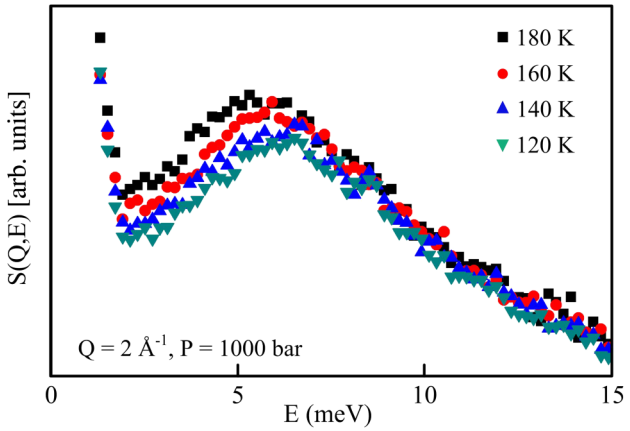

FIG. 5 (color online). The measured spectra of the confined water system at $T = 120$, 140, 160, and 180 K under $P = 1000$ bar. (Measured at CNCS.)

below, $\langle \tau_T \rangle$ transforms from ("strong") Arrhenius behavior to ("fragile") super-Arrhenius behavior [11]. The strong-to-fragile crossover causes the quasielastic peak to greatly broaden within a small T increase. On the other hand, there is little evidence of abrupt changes in the shape of the boson peak on crossing T_W. Considering these facts, we conclude that the parallel between the emergence or disappearance of the boson peak and the FSC is mainly due to the drastic change of the quasielastic component in the spectrum induced by the FSC at the Widom line. On the other hand, the change in the boson peak itself contributes not so much to this parallel. This conclusion can be illustrated more clearly in Fig. 1(b2): for $T = 200$ and 210 K, temperatures in the strong region, the quasielastic peak is narrow and the boson peak is visible. However, for $T = 220$ K, which is in the fragile region and is roughly 10 K higher than T_W, the quasielastic peak is significantly broadened and its wing, which is greatly strengthened, "buries" the boson peak.

From Fig. 3, it is evident that above ~1600 bar, the slope of the $T_B(P)$ profile is different from the slope below ~1600 bar: the positions of $T_B(P)$ under $P = 2000$ and 2400 bar deviate considerably from the extrapolation of the lower pressure cases. This deviation, though not a definitive proof, is consistent with the previous statement that the Widom line ends between 1500 and 2000 bar [11]. Since if the Widom line continues to develop at pressures higher than 2000 bar, then due to the relation between $T_B(P)$ and the Widom line, the profile of $T_B(P)$ will smoothly develop at higher pressures in a fashion similar to that of the Widom line. In the LLCP hypothesis, the Widom line ends at the LLCP, which produces a singularity. In this sense, the profile of $T_B(P)$ is not necessarily smooth at the critical pressure. Thus, one may estimate the critical pressure (if it exists) by finding the intersection point of the extrapolations of the two points at $P = 2000$ and 2400 bar and of the two points at $P = 1200$ and 1500 bar. As shown in Fig. 3, the critical pressure estimated in this way is 1592 bar, which is consistent with the result of 1600 ± 400 bar obtained by detecting the end pressure of the FSC [11].

Figure 4(a) shows that the frequency of the boson peak Ω slightly increases as T increases within $200\ \text{K} < T < 230\ \text{K}$. However, from Fig. 5, one can find that within $120\ \text{K} < T < 180\ \text{K}$, Ω decreases as T increases. (Since we do not have the RCM parameters for confined water in this T range, we cannot perform a quantitative analysis. However, in this T range, the quasielastic peak in the spectrum is very narrow and will not affect the shape of the inelastic spectrum too much.) This result suggests that a frequency minimum exists between about 180 and 200 K. Notice that the density of water also exhibits a minimum in the same region [14]. In addition, Ω tends to increase as the pressure increases. These facts suggest that Ω and the density of the deeply cooled water are positively correlated. The width of the boson peak (Γ) also exhibits such a behavior. In fact, similar phenomena were also observed in other amorphous materials [25]. This result is of particular importance to water. In the LLCP hypothesis, the order parameter to distinguish the LDL and HDL phases is just the density. With this in mind, and considering that a change in the local structure can also shift the boson peak [25], one may distinguish the hypothetical LDL and HDL phases in deeply cooled water by looking at the shape of the boson peak. In other words, the frequency or the width of the boson peak may exhibit abrupt change as the water transforms between LDL and HDL, due to significant differences in density and local structure of the different sides of the hypothetical first order transition line between LDL and HDL [15,26].

The research at MIT was supported by DOE Grant No. DE-FG02-90ER45429. K. H. L. is sponsored by the National Science Council of Taiwan, "New Partnership Program for the Connection to the Top Labs in the World." The work at NIST was supported in part by the National Science Foundation under Agreement No. DMR-0944772. The work at ORNL was supported by the Scientific User Facilities Division, Office of Basic Energy Sciences, and U.S. Department of Energy. We thank Professor Li Liu for providing the RCM parameters.

*Corresponding author.
sowhsin@mit.edu

[1] A. I. Chumakov, G. Monaco, A. Monaco *et al.*, Phys. Rev. Lett. **106**, 225501 (2011).
[2] B. Frick and D. Richter, Science **267**, 1939 (1995).
[3] H. Shintani and H. Tanaka, Nat. Mater. **7**, 870 (2008).
[4] S.-H. Chen *et al.*, AIP Conf. Proc. **982**, 39 (2008).
[5] S.-H. Chen, X.-Q. Chu, M. Lagi, C. Kim, Y. Zhang, A. Faraone, J. B. Leao, E. Fratini, P. Baglioni, and F. Mallamace (unpublished).

[6] P. Kumar, K. T. Wikfeldt, D. Schlesinger, L. G. M. Pettersson, and H. E. Stanley, Sci. Rep. **3**, 1980 (2013).
[7] L. Xu, P. Kumar, S. V. Buldyrev, S.-H. Chen, P. H. Poole, F. Sciortino, and H. E. Stanley, Proc. Natl. Acad. Sci. U.S.A. **102**, 16558 (2005).
[8] J. R. D. Copley and J. C. Cook, Chem. Phys. **292**, 477 (2003).
[9] G. Ehlers, A. A. Podlesnyak, J. L. Niedziela, E. B. Iverson, and P. E. Sokol, Rev. Sci. Instrum. **82**, 085108 (2011).
[10] R. T. Azuah, L. R. Kneller, Y. Qiu, P. L. W. Tregenna-Piggott, C. M. Brown, J. R. D. Copley, and R. M. Dimeo, J. Res. Natl. Inst. Stand. Technol. **114**, 341 (2009).
[11] L. Liu, S.-H. Chen, A. Faraone, C.-W. Yen, and C.-Y. Mou, Phys. Rev. Lett. **95**, 117802 (2005).
[12] D. Liu, Y. Zhang, C.-C. Chen, C.-Y. Mou, P. H. Poole, and S.-H. Chen, Proc. Natl. Acad. Sci. U.S.A. **104**, 9570 (2007).
[13] Y. Zhang, A. Faraone, W. A. Kamitakahara, K.-H. Liu, C.-Y. Mou, J. B. Leão, S. Chang, and S.-H. Chen, Proc. Natl. Acad. Sci. U.S.A. **108**, 12206 (2011).
[14] K.-H. Liu, Y. Zhang, J.-J. Lee, C.-C. Chen, Y.-Q. Yeh, S.-H. Chen, and C.-Y. Mou, J. Chem. Phys. **139**, 064502 (2013).
[15] P. H. Poole, F. Sciortino, U. Essmann, and H. E. Stanley, Nature (London) **360**, 324 (1992).
[16] C. B. Bertrand, Y. Zhang, and S.-H. Chen, Phys. Chem. Chem. Phys. **15**, 721 (2013).
[17] G. L. Squires, *Introduction to the Theory of Thermal Neutron Scattering* (Cambridge University Press, Cambridge, England, 1978), p. 68.
[18] S.-H. Chen, C. Liao, F. Sciortino, P. Gallo, and P. Tartaglia, Phys. Rev. E **59**, 6708 (1999).
[19] L. Liu, S.-H. Chen, A. Faraone, C.-W. Yen, C.-Y. Mou, A. I. Kolesnikov, E. Mamontov, and J. Leão, J. Phys. Condens. Matter **18**, S2261 (2006).
[20] B. Fåk and B. Dorner, Physica (Amsterdam) **234B**, 1107 (1997).
[21] G. Ruocco and F. Sette, J. Phys. Condens. Matter **11**, R259 (1999).
[22] F. Sette, M. H. Krisch, C. Masciovecchio, G. Ruocco, and G. Monaco, Science **280**, 1550 (1998).
[23] See the Supplemental Material at http://link.aps.org/supplemental/10.1103/PhysRevLett.112.237802 for descriptions of the sample, instrument, model, and data analysis used in this study.
[24] A full DHO curve contains two asymmetric peaks that reside in the Stokes and anti-Stokes sides of the spectrum. They overlap each other so that the position of the maximum of the curve is not equal to the frequency of the DHO model.
[25] A. Monaco, A. I. Chumakov, G. Monaco, W. A. Crichton, A. Meyer, L. Comez, D. Fioretto, J. Korecki, and R. Rüffer, Phys. Rev. Lett. **97**, 135501 (2006).
[26] A. K. Soper and M. A. Ricci, Phys. Rev. Lett. **84**, 2881 (2000).